NASA TECHNICAL NOTE

NASA TN D-3563

C.1

NASA TN D-3563

ATTENUATION OF SINUSOIDAL DISTURBANCES IN NONVISCOUS LIQUID FLOWING IN A LONG LINE WITH DISTRIBUTED LEAKAGE

by Robert J. Blade and Carl M. Holland

Lewis Research Center
Cleveland, Ohio

NATIONAL AERONAUTICS AND SPACE ADMINISTRATION • WASHINGTON, D. C. • AUGUST 1966

NASA TN D-3563

ATTENUATION OF SINUSOIDAL DISTURBANCES IN NONVISCOUS LIQUID FLOWING IN A LONG LINE WITH DISTRIBUTED LEAKAGE

By Robert J. Blade and Carl M. Holland

Lewis Research Center
Cleveland, Ohio

NATIONAL AERONAUTICS AND SPACE ADMINISTRATION

For sale by the Clearinghouse for Federal Scientific and Technical Information
Springfield, Virginia 22151 – Price $2.00

ATTENUATION OF SINUSOIDAL DISTURBANCES IN NONVISCOUS LIQUID FLOWING IN A LONG LINE WITH DISTRIBUTED LEAKAGE

by Robert J. Blade and Carl M. Holland

Lewis Research Center

SUMMARY

Sinusoidal disturbances from 0.5 to 82 cps superimposed on the flow of a nonviscous liquid were attenuated to design values in a 66-foot-long (20.1 m) line. The disturbances were attenuated by placing shunt assemblies that simulate distributed leakage along the line. Experimental values of the attenuation constant were determined and compared with the design values that were obtained from analogous electrical transmission line theory. The results showed that sinusoidal perturbations at a given frequency can be attenuated to a design value by using shunt assemblies and that theory and experiment agreed well.

INTRODUCTION

Because acoustic pressure and flow perturbations are often of importance in the operation of various fluid systems, the Lewis Research Center has been involved in a general experimental research program to determine the effects of acoustic disturbances in flowing-liquid systems. Transfer functions for acoustic disturbances superimposed on the mean flow of liquid propellant in long lines of several geometric networks are reported in references 1 to 3. A study of the attenuation constant associated with sinusoidal perturbations superimposed on the mean laminar flow of a viscous liquid in a long line is described in reference 4.

Pressure and flow perturbations in long liquid-filled lines are often a contributing element toward instabilities in liquid rockets and hydraulic control systems. For example, longitudinal instabilities in liquid rockets have resulted from a closed-loop coupling of disturbances in the propellant feed lines, engines, and structure. A convenient method of stabilizing these systems is to attenuate sufficiently the pressure and flow perturbations in these lines.

This investigation was conducted to determine the efficacy of attenuating to design

values sinusoidal disturbances superimposed on the mean flow of a nonviscous liquid (the type of fluid often used in practice) in a long line by means of shunt assemblies placed along the test line. These assemblies were closely spaced relative to disturbance wavelength. Experimental values of the attenuation constant were determined and compared with the values obtained from the analogous electrical transmission line equations for the zero distributed series disturbance-resistance and nonzero disturbance-resistance and nonzero distributed leakage.

Attenuation studies were conducted with JP-4 fuel flowing in a 66-foot-long (20.1 m) stainless-steel line (1 in. o.d. or 2.54×10^{-2} m). The line was firmly supported at both ends and contained 33 equally spaced shunt assemblies. Two types of shunt assemblies were tested. One type was essentially a porous-metal disk. The other type was essentially 21 small-diameter tubes (lossy tubes) arranged in parallel. Flow was modulated at frequencies from 0.5 to 82 cps by means of an electrohydraulic servothrottle. Mean line pressures ranged from 75 to 155 pounds per square inch gage (5.17×10^{5} to 1.07×10^{6} N/m^2 gage), and mean line flow ranged from 7 to 9.4 feet per second (2.1 to 2.9 m/sec).

APPARATUS

Flow System

The essential parts of the open-loop pumped-return flow system used in the experiment are shown in figure 1(a). The liquid (JP-4 fuel) was forced through the test line by a gear pump, and the mean flow rate was measured by means of a rotameter. A heat exchanger in the fluid supply tank maintained the fluid at $79^{\circ}\pm3^{\circ}$ F for the porous-metal shunt element studies and at $85^{\circ}\pm3^{\circ}$ F for the lossy-tube shunt-element studies. Hydraulic accumulators were placed between the pump and the test line to provide steady supply pressure. The discharge from the test line was submerged in a constant-height vented tank. Fluid was returned to the supply tank by intermittent operation of the return pump.

Test Line

The test line consisted of a 66-foot-long (20.1 m) stainless-steel tube with a 1.00-inch (2.54×10^{-2} m) outside diameter and a 0.065-inch-thick (1.6×10^{-3} m) wall, which was fitted with 33 equally spaced shunt assemblies as shown in figure 1(b). The test line rested horizontally on transverse wires spaced at 2-foot (0.6 m) intervals. The upstream and downstream ends of the tube were firmly supported in order to avoid line vibration. The downstream end was terminated in an orifice plate containing 34 holes of 0.040-inch

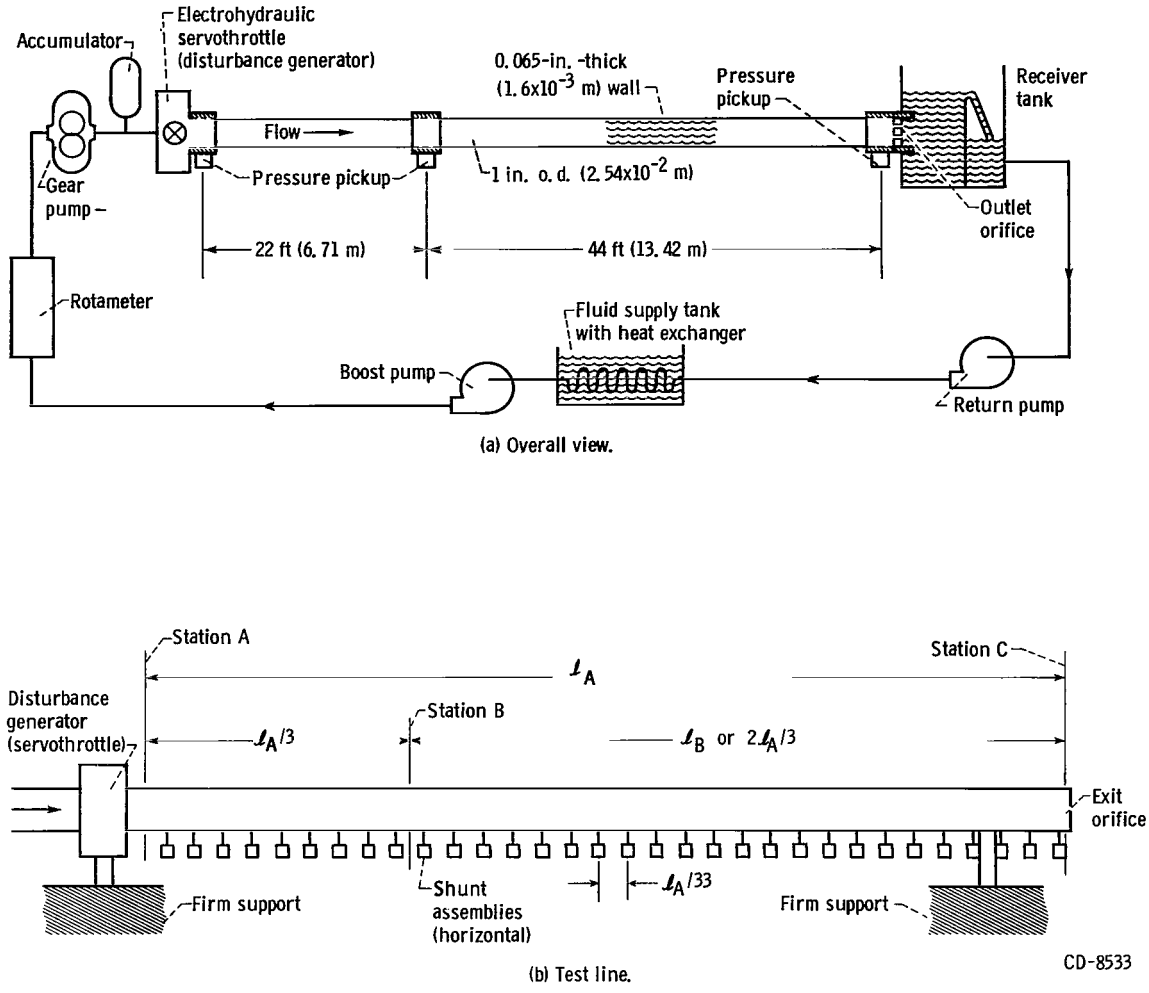

Figure 1. - Schematic drawing of flow system.

(1.0×10^{-3} m) diameter. The range of run-averaged dimensionless downstream admittance for the runs was from 0.95 to 1.4. (Dimensionless downstream admittance is the ratio of downstream admittance to characteristic admittance of the line.)

Shunt Assemblies

Schematic drawings of the two types of shunt assemblies used are shown in figure 2. For both types of assemblies, an accumulator (total volume, 10 $in.^3$ or 1.64×10^{-4} m^3) was used as a sink and source of liquid. Provision was made for bleeding to ensure that the fluid flowing through the shunt element was JP-4 fuel.

The porous-metal shunt element was a commercial bronze, porous-metal disk (Morain Products Grade 4 Porex) 0.0156 foot (4.75×10^{-3} m) in diameter (the same as

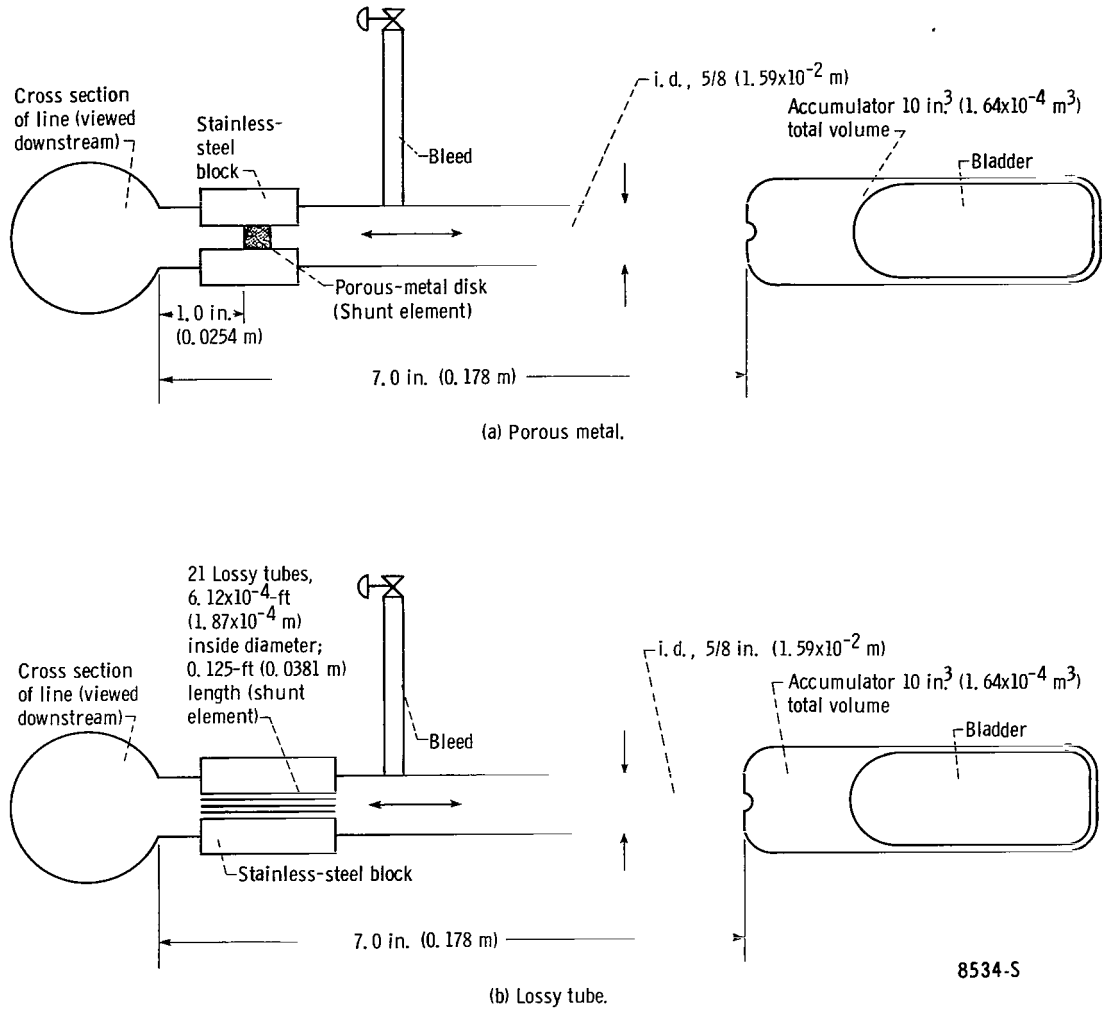

Figure 2. - Typical shunt assemblies.

the flow diameter) and 0.0208 foot (6.34×10^{-3} m) thick. It was mounted in a hole drilled through a stainless-steel block.

The lossy-tube shunt element was essentially 21 parallel Inconel tubes of 0.125-foot (3.81×10^{-2} m) length and 6.12×10^{-4} foot (1.87×10^{-4} m) inner diameter mounted in a 6.55×10^{-3}-foot-diameter (2.00×10^{-3} m) hole drilled through a stainless-steel block. The volume between these lossy tubes was filled with solder at both ends of the stainless-steel block.

Flow Disturbance Generator

Sinusoidal perturbations of flow and pressure (from 0.5 to 82 cps) were induced in the system by means of an electrohydraulic servothrottle located at the upstream end of the test line. The throttle was oscillated sinusoidally (by a master oscillator) about a partly open mean position in response to an alternating voltage. The amplitude of the

sinusoidal pressure perturbations was of the order of 10 pounds per square inch (7×10^4 N/m^2).

Instrumentation

Commercial flush-diaphragm pressure transducers were used to measure pressure perturbations at stations A, B (chosen for convenience), and C (fig. 1(b)). The transducers with their associated electronic equipment were statically calibrated to determine their gain factors. The inphase and quadrature components (relative to the master servothrottle oscillator) of the pressure perturbations were determined by means of a commercial transfer-function analyzer, as was done for previous studies (refs. 1, 2, or 4).

PROCEDURE

Test

Each accumulator associated with the shunt assemblies was charged to about 80 percent of the desired mean line pressure. Then the flow system was operated until the flow rate, temperature, and line pressure had stabilized. The mean flow rate, the pressures at stations A and C, and the liquid temperature adjacent to the orifice in the receiver tank were recorded. The servothrottle was operated at a series of frequencies. The amplitude of the throttle-area variation was maintained constant over the entire range of frequencies for each run and was small relative to the mean open area in order to avoid nonlinear effects. At each frequency the values of the inphase and quadrature components of the pressure perturbations at stations A, B, and C (fig. 1(b)) were recorded. The mean pressure drop across the downstream orifice was constant during each test run but was changed from run to run (by changing the mean line pressure) to vary the orifice impedance.

Data Analysis

The following quantities were computed from the experimental data for each frequency:

(1) Attenuation constant, α, Np/ft

(2) Phase constant, β, rad/ft

(3) Complex dimensionless admittance at station C, z/Z_C (fig. 1(b))

(All symbols are defined in appendix A.)

The values of these quantities at each frequency were obtained from the following (complex) equations:

$$\frac{P_A}{P_C} = \cosh(\alpha + j\beta)\ell_A + \frac{z}{Z_C}\sinh(\alpha + j\beta)\ell_A \tag{1}$$

$$\frac{P_B}{P_C} = \cosh(\alpha + j\beta)\ell_B + \frac{z}{Z_C}\sinh(\alpha + j\beta)\ell_B \tag{2}$$

This pair of equations was obtained from the well-known pressure transfer function for damped sinusoidal one-dimensional waves in a uniform medium. (This transfer function is considered herein to be the defining relation for α.) Equations (1) and (2) were solved numerically on a digital computer by a procedure described in reference 4. The necessary input data were (1) the six measured values of the inphase and quadrature components of the pressure disturbance amplitudes at stations A, B, and C (fig. 1(b)), that is, P_A, P_B, and P_C; and (2) the distance in feet between stations A and C, ℓ_A, and between stations B and C, ℓ_B.

RESULTS AND DISCUSSION

The experimental results were compared with analytical values obtained from the analogous electrical transmission line equation for nonzero distributed leakage and zero distributed series disturbance-resistance. As shown in appendix B, the analytical relations for the attenuation constant and the phase constant, respectively, are given by the positive roots of

$$\alpha_i = \left[\frac{\omega L_D}{2}\left(\sqrt{\omega^2 K_D^2 + G_D^2} - \omega K_D\right)\right]^{1/2} \tag{3}$$

and

$$\beta = \left(\omega^2 K_D L_D + \alpha_i^2\right)^{1/2} \tag{4}$$

For the porous-metal shunt-element studies, the effective distributed leakage G_D has the constant value given by

$$G_D = \frac{1}{R_s} \frac{n}{\ell_A} \tag{5}$$

and K_D and L_D have the constant values (see appendix C) for zero shunt admittance. For the lossy-tube shunt-element studies, G_D and K_D are frequency dependent as given by

$$G_D = \frac{n}{\ell_A} \quad \frac{R_T}{R_T^2 + \omega^2 L_T^2} \tag{6}$$

$$K_D = C_D - \frac{n}{\ell_A} \quad \frac{L_T}{R^2 + \omega^2 L^2} \tag{7}$$

and L_D again has its zero-leakage constant value. (Appendix C contains the numerical values of the parameters.)

The experimental values obtained for both the porous-metal and the lossy-tube shunt-element studies are presented in figures 3 to 5 for various values of mean line pressure. These experimental values were obtained by the method previously described in the section PROCEDURE. The analytical results (curves) are presented for comparison. The curves were obtained by use of equations (3) to (7). Curves for frequencies less than 7 cps are shown as dashed lines because, for these frequencies, the distributed series disturbance-resistance may be significant in the computation of the attenuation and phase constants (appendix B).

The attenuation constant α (in Np/ft) is presented in figure 4 as a function of the perturbation frequency. The agreement between the analytical and experimental results is considered good. The experimental data exhibit some scatter and slight variations with mean line pressure. Because of the high accuracy requirements, however, these effects can be attributed to limits of accuracy of the instrumentation.

A comparison of the results for the porous-metal and lossy-tube shunt-element studies in figure 3 shows the effect of inertive impedance in the shunt elements. For the porous-metal element studies, α was essentially constant for frequencies greater than 30 cps, while for the lossy-tube elements, α decreased with increasing frequency over this frequency range. This behavior occurred because for the porous-metal elements G_D (eq. (5)) and K_D were independent of frequency; whereas for the lossy-tube elements, the inertance had a greater effect on decreasing the value of G_D (eq. (6)) than increasing K_D (eq. (7)).

Equation (3) shows that, for a fixed frequency and an essentially constant value of

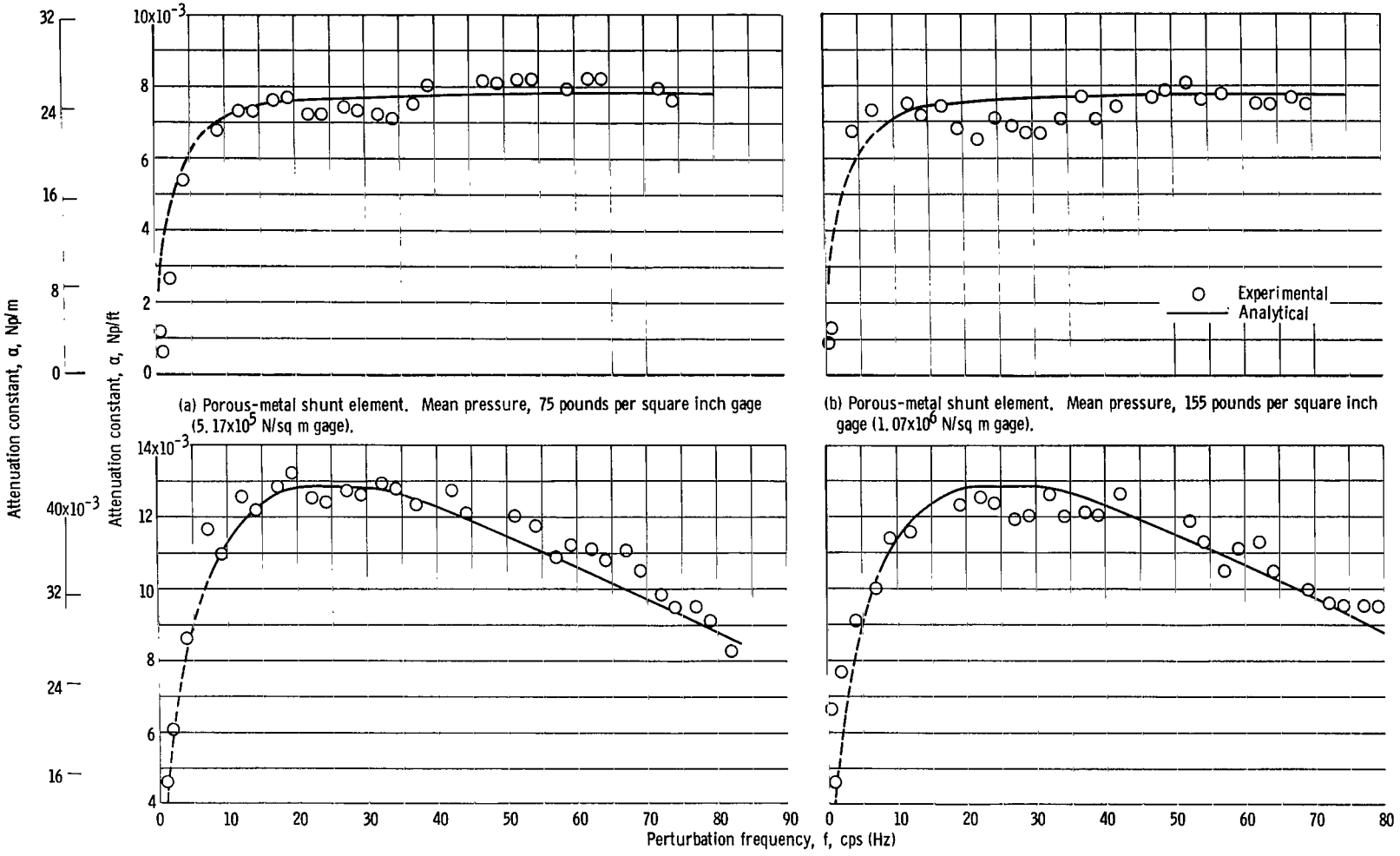

(a) Porous-metal shunt element. Mean pressure, 75 pounds per square inch gage (5.17×10^5 N/sq m gage).

(b) Porous-metal shunt element. Mean pressure, 155 pounds per square inch gage (1.07×10^6 N/sq m gage).

(c) Lossy-tube shunt element. Mean pressure, 97 pounds per square inch gage (6.69×10^5 N/sq m gage).

(d) Lossy-tube shunt element. Mean pressure, 138 pounds per square inch gage (9.51×10^5 N/sq m gage).

Figure 3. - Variation of attenuation constant with perturbation frequency.

K_D, α decreases as G_D decreases. If the radius of each lossy tube were sufficiently small (inequality, (eq. (C1)), α would not decrease with increasing frequency for the lossy-tube shunt-element case over the frequency range of consideration.

In order to interpret the results obtained for α more easily, the attenuation constant is presented in figure 4 in terms of $e^{-100\alpha}$. This term is the ratio of downstream to upstream pressure for a wave traveling in the downstream direction for two points along the line that are separated by 100 feet (30.5 m). For the same test line with no shunt elements (ref. 1), the attenuation is negligible. The results of figure 4 indicate that (except for the lower frequencies) the attenuation was approximately 55 percent for a 100-foot (30.5 m) line for the porous-metal shunt-element studies, and was an average of approximately 65 percent for a 100-foot (30.5 m) line for the lossy-tube shunt-element studies. There is good agreement between the design (analytical) and experimental values. Therefore, it has been experimentally shown that sinusoidal perturbations in a fluid flowing in a long line can be attenuated to a design value. High values of attenuation may be realized by increasing the value of the effective distributed leakage G_D (eq. (3)). Equations (5) and (6) show that the value of G_D can be indreased by (1) decreasing the lumped resistance of each shunt assembly R_S (or R_T) (see appendix C), (2) increasing the number of shunt assemblies per unit length of main line n/ℓ_A, or (3) decreasing the inertance of each shunt assembly L_T (lossy-tube shunt-element case).

Analytical and experimental values of the phase constant β are presented in figure 5 in terms of the ratio of phase constant to perturbation frequency as a function of frequency. The analytical and experimental results agree very well.

As in reference 4, a comparison of the experimental values of the complex dimensionless downstream admittance z/Z_C (eqs. (1) and (2)) with that calculated from the analogous electrical transmission line equations (ref. 5) and the resistance of the downstream orifice showed no serious discrepancies. (Magnitudes agreed within ±10 percent, and angles agreed within $\pm 10^{\circ}$.) This agreement confirms the implied assumption that the data analysis gave the roots of interest.

No strong conclusion was reached as to which of the two types of tested shunt elements is more advantageous. During the determination of the leakage of the porous-metal shunt elements, it was noted that the elements could be partly clogged by dirt particles rather easily. This fact may limit the practical application of porous-metal shunt elements. From the analysis of the lossy-tube shunt element, however, (eq. (3) and appendix C) the attenuation constant was found to be very sensitive to the diameter of the lossy tubes. A 1-percent increase in the diameter of each lossy tube would cause about a 4 percent increase in the attenuation constant. Therefore, the lossy tubes must be constructed carefully in order to obtain the design value of the attenuation constant.

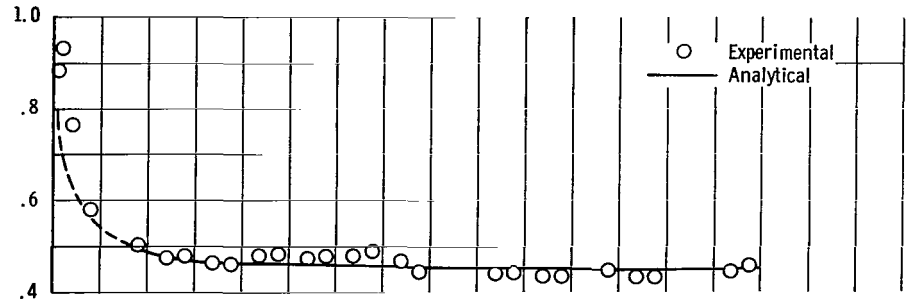

(a) Porous-metal shunt element. Mean pressure, 75 pounds per square inch gage (5.17×10^5 N/sq m gage).

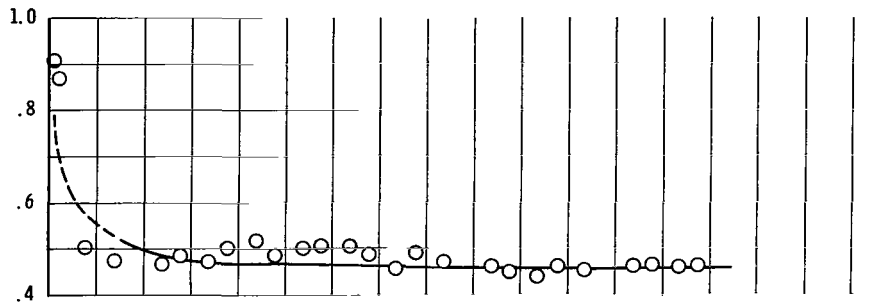

(b) Porous-metal shunt element. Mean pressure, 155 pounds per square inch gage (1.07×10^6 N/sq m gage).

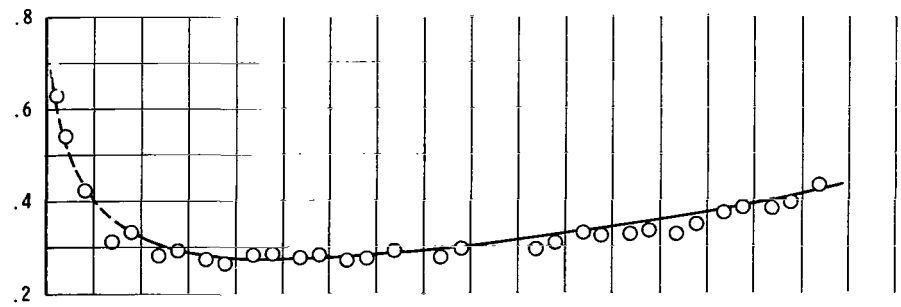

(c) Lossy-tube shunt element. Mean pressure, 97 pounds per square inch gage (6.69×10^5 N/sq m gage).

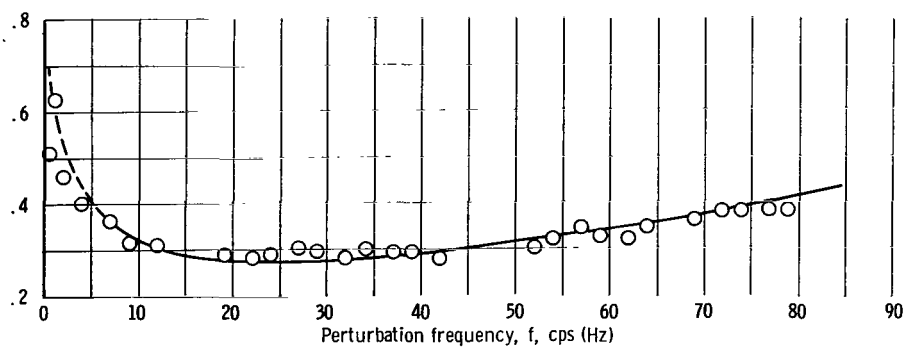

(d) Lossy-tube shunt element. Mean pressure, 138 pounds per square inch gage (9.51×10^5 N/sq m gage).

Figure 4. - Effect of frequency on attenuation, expressed as pressure amplitude ratio $e^{-100\alpha}$, (where α is attenuation constant.

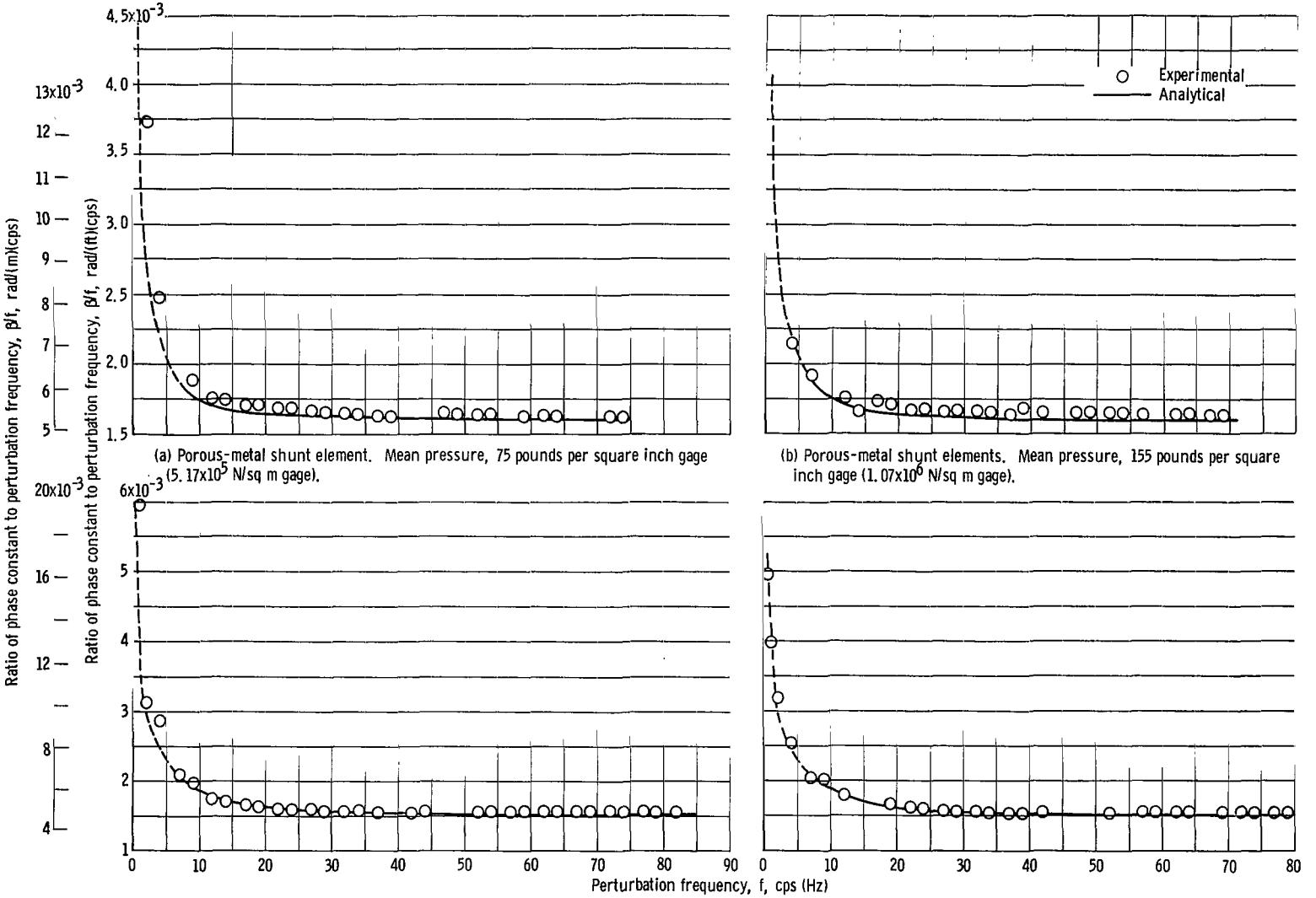

(a) Porous-metal shunt element. Mean pressure, 75 pounds per square inch gage (5.17×10^5 N/sq m gage).

(b) Porous-metal shunt elements. Mean pressure, 155 pounds per square inch gage (1.07×10^6 N/sq m gage).

(c) Lossy-tube shunt element. Mean pressure, 97 pounds per square inch gage (6.69×10^5 N/sq m gage).

(d) Lossy-tube shunt element. Mean pressure, 138 pounds per square inch gage (9.51×10^5 N/sq m gage).

Figure 5. - Effect of frequency on ratio of phase constant to perturbation frequency.

SUMMARY OF RESULTS

The results of this study show that (1) shunt assemblies closely spaced relative to sinusoidal disturbance wavelength can effectively attenuate to design values sinusoidal perturbations at a given frequency superimposed on the mean flow of a fluid in a long line, and that (2) the analogous electrical transmission line theory adequately predicts the attenuation constant when series disturbance-resistance is negligible.

Lewis Research Center,
National Aeronautics and Space Administration,
Cleveland, Ohio, April 27, 1966,
129-02-04-06-22.

APPENDIX A

SYMBOLS

A cross-sectional area of a line, ft^2 (m^2)

a isentropic ($R_D = 0$) sonic speed in the line with zero leakage, $\sqrt{1/C_D L_D}$, ft/sec (m/sec)

C_D distributed shunt compliance of the main line not including the reactance (negligible for porous-metal shunt elements) due to shunt assemblies, ft^4/lb (m^4/N)

d length of each lossy tube, ft (m)

f frequency, cps (hertz)

G_D effective distributed leakage of the line, $ft^4/lb\text{-}sec$ ($m^4/N\text{-}sec$)

h length of line, ft (m)

I_x defined by eq. (C20)

I_y defined by eq. (C21)

j $\sqrt{-1}$

K lumped compliance, ft^5/lb (m^5/N)

K_D effective distributed compliance of the line (C_D for porous-metal shunt element case), ft^4/lb (m^4/N)

k constant defined by eq. (B7)

ℓ tube length from any point to station C (fig. 1(b)), ft (m)

L lumped inertance, $lb\text{-}sec^2/ft^5$ ($N\text{-}sec^2/m^5$)

L_D distributed series inertance of the line, $lb\text{-}sec^2/ft^6$ ($N\text{-}sec^2/m^6$)

L_T distributed specific inertance of each lossy tube, $lb\text{-}sec^2/ft^4$ ($N\text{-}sec^2/m^4$)

M constant defined by eq. (C5)

n number of shunt assemblies (33)

P complex amplitude of perturbation pressure, lb/ft^2 (N/m^2)

ΔP pressure amplitude drop across length of lossy tube (complex), lb/ft^2 (N/m^2)

p pressure, lb/ft^2 (N/m^2)

Δp pressure drop between stations A and C (fig. 1(b)), lb/ft^2 (N/m^2)

R lumped disturbance-resistance, $lb\text{-}sec/ft^5$ ($N\text{-}sec/m^5$)

R_D distributed series disturbance-resistance of the line, $lb\text{-}sec/ft^6$ ($N\text{-}sec/m^6$)

R_T distributed specific disturbance-resistance of each lossy tube, $lb\text{-}sec/ft^4$ ($N\text{-}sec/m^4$)

r inner radius of each lossy tube, ft (m)

U complex amplitude of sinusoidal-perturbation velocity in axial direction of each lossy tube averaged over a cross-sectional area of each tube, ft/sec (m/sec)

V complex amplitude of sinusoidal-perturbation volume flow rate in axial direction for each lossy tube, $U\pi r^2$, ft^3/sec (m^3/sec)

v volume flow rate in the line, ft^3/sec (m^3/sec)

Y_D effective distributed shunt admittance of the line (complex), $ft^4/lb\text{-}sec$ ($m^4/N\text{-}sec$)

Z lumped impedance, $lb\text{-}sec/ft^5$ ($N\text{-}sec/m^5$)

Z_C impedance at station C (fig. 1(b)) looking downstream (complex), (approximately real for this experiment), $lb\text{-}sec/ft^5$ ($N\text{-}sec/m^5$)

Z_D distributed series impedance of line (complex), $lb\text{-}sec/ft^6$ ($N\text{-}sec/m^6$)

z characteristic impedance of the line (complex), $lb\text{-}sec/ft^5$ ($N\text{-}sec/m^5$)

α attenuation constant, nepers/ft (Np/m)

β phase constant, rad/ft (rad/m)

γ ratio of specific heats, dimensionless

δ defined by eq. (B14)

μ absolute viscosity, $lb\text{-}sec/ft^2$ ($N\text{-}sec/m^2$)

ξ coordinate in axial direction of each lossy tube, ft (m)

ρ density of liquid, $slugs/ft^3$ (kg/m^3)

σ maximum radius of tubes in a series-parallel combination equivalent to a typical porous-metal shunt element, ft (m)

ω frequency, $2\pi f$, rad/sec

Ω volume of gas in shunt assembly accumulator, ft^3 (m^3)

Subscripts:

A, B, C reference stations located as shown in fig. 1(b)

g shunt-accumulator condition when charged

i case of $R_D = 0$

m mean value

s porous-metal shunt assembly

T lossy-tube shunt element

0 zeroth order

1 first order

APPENDIX B

DERIVATION OF ANALYTICAL ATTENUATION AND PHASE CONSTANTS

Attenuation of pressure disturbances due to factors such as heat exchange, absorption of acoustic energy by the main tube wall, molecular exchanges of energy, and impurities (ref. 6) are neglected in the following derivation of the attenuation and phase constants.

DERIVATION OF EQUATIONS (3) AND (4) OF THE REPORT

By analogy with electrical transmission line theory (ref. 6), the propagation constant is given by (ref. 5)

$$\alpha + j\beta = \sqrt{Z_D Y_D} \tag{B1}$$

where the effective distributed shunt admittance of the line is

$$Y_D = G_D + j\omega K_D \tag{B2}$$

and, for the case of zero distributed series disturbance-resistance ($R_D = 0$), the distributed series impedance is

$$Z_D = j\omega L_D \tag{B3}$$

Substituting equations (B2) and (B3) into equation (B1), squaring the result, and equating the real and imaginary parts yield

$$\beta^2 - \alpha_i^2 = \omega^2 L_D K_D \tag{B4}$$

and

$$2\beta\alpha_i = \omega L_D G_D \tag{B5}$$

Solving equation (B4) for β^2 and taking the positive square root of the result gives equation (4) of the text.

In order to find the expression for α_i, equation (B5) is solved for β and the result is substituted into equation (B4). This procedure gives, after the terms are rearranged,

$$\alpha_i^4 + \omega^2 L_D K_D \alpha_i^2 - \left(\frac{\omega}{2} L_D G_D\right)^2 = 0 \tag{B6}$$

Solving this quadratic equation for α_i^2 and taking the positive square root of the result and rearranging terms give equation (3) of the text for the attenuation constant α_i.

SUBSTANTIATION FOR HIGHER FREQUENCIES OF ASSUMPTION THAT $R_D = 0$

The equation for the distributed series-disturbance resistance R_D of the line is obtained from the equation for the pressure drop in a line for turbulent flow as follows:

$$\Delta P = kv^2 \tag{B7}$$

It is assumed that

$$R_D = \frac{1}{\ell_A} \frac{d(\Delta P)}{dv} \tag{B8}$$

From equations (B7) and (B8)

$$R_D = \frac{2(\Delta P)}{v\ell_A} \tag{B9}$$

This equation is often used for small disturbances superimposed on turbulent mean flow instead of a rigorously derived equation. Another equation that might be used to evaluate R_D for turbulent mean flow is the one for laminar disturbance flow (R_T/A, eq. (C19)). Of these two equations, however, equation (B9) gave the greatest values of R_D for this experiment. Equation (B9) is, therefore, used as the worst case equation.

For the nonzero values of distributed series line, disturbance-resistance, equations (B1) and (B2) are valid, but the following equation for Z_D is the more general equation instead of equation (B3):

$$Z_D = R_D + j\omega L_D \tag{B10}$$

Following the procedure that led to α^2 for the case of $R_D = 0$ presented previously gives

$$\alpha^2 = \frac{1}{2}\left[R_D G_D - \omega^2 L_D K_D + \omega L_D \sqrt{\omega^2 K_D^2 + G_D^2}\left(1 + \frac{R_D^2}{\omega^2 L_D^2}\right)^{1/2}\right] \tag{B11}$$

The effect of R_D for the porous-metal shunt element case is now examined. The maximum value of R_D for the runs of this case (obtained from eq. (B9) with use of mean state data) is 9.76×10^2 (5.41×10^6 N-sec/m^6) pound-second per foot^6. The values of G_D, L_D, and K_D are given in appendix C.

Using the numerical values of these line parameters and a frequency of 7 cps or greater gives

$$\frac{R_D^2}{\omega^2 L_D^2} < 0.004 \tag{B12}$$

Neglecting this term in equation (B11), taking the square root of the result, and rearranging terms give

$$\alpha \approx \left[\frac{\omega L_D}{2}\left(\sqrt{\omega^2 K_D^2 + G_D^2} - \omega K_D\right)\right]^{1/2}(1 + \delta)^{1/2} \tag{B13}$$

where the remaining correction term for distributed series disturbance-resistance is

$$\delta = \frac{R_D G_D}{\omega L_D\left(\sqrt{\omega^2 K_D^2 + G_D^2} - \omega K_D\right)} = \frac{R_D G_D}{2\delta_i^2} \tag{B14}$$

(See eq. (3) of the text.) Evaluating δ (always positive) for test frequencies of 7 cps or greater gives

$$\delta < 0.14 \tag{B15}$$

From inequality (B15) and a binomial expansion of the factor $(1 + \delta)^{1/2}$ in equation (B13), it follows that

$$\alpha \approx \left[\frac{\omega L_D}{2}\left(\sqrt{\omega^2 K_D^2 + G_D^2} - \omega K_D\right)\right]^{1/2}\left(1 + \frac{1}{2}\delta\right) \tag{B16}$$

The bracketed term raised to the one-half power is the exact attenuation constant for zero distributed series disturbance-resistance R_D (eq. (3)). The magnitude of the correction term $\left(\frac{1}{2}\delta\right)$ in equation (B16) for the nonzero value of R_D is less than 7 percent for frequencies equal to or greater than 7 cps over the frequency range of the experiment. This error is within the limits of accuracy of the experiment. Therefore, R_D can be neglected for these frequencies.

In computing the phase constant β for tested frequencies of 7 cps or higher, the magnitude of the maximum correction factor for the nonzero value of R_D can be shown to be negligible by a similar procedure.

This method applied to the lossy-tube shunt-element case showed that R_D can also be neglected for tested frequencies of 7 cps or greater.

APPENDIX C

DISTRIBUTED LINE IMPEDANCE DUE TO SHUNT ASSEMBLIES

The acoustic line used in this study is treated as an analogous electrical transmission line, as is generally done. The acoustic analogous of electrical voltage, current, inductance, and capacitance are pressure, volume flow rate, inertance, and compliance, respectively, (ref. 6).

Before the two types of shunt assemblies are analyzed separately, it is shown that each can be treated as distributed along the main line. This distribution is established by proving that there is at least one shunt assembly per quarter wavelength (ref. 6) as follows. For a perturbation frequency of 82 cps (the maximum experimental value) and an approximate wave propagation velocity of 3920 feet per second (1195 m/sec) (isentropic zero-leakage value of acoustic velocity), the minimum sinusoidal disturbance quarter wave-length for the experimental study was 12 feet (3.66 m). The shunt assemblies were placed 2 feet (6.1×10^{-1} m) apart. Because the minimum number of shunt assemblies per quarter wavelength over the frequency range of the experiment was at least 6, the shunt assemblies can be regarded as distributed.

POROUS-METAL SHUNT ASSEMBLIES

Impedance of Porous-Metal Shunt Element

The impedance of a porous-metal shunt element is shown to be approximately resistive and frequency independent. Laminar disturbance flow through a porous-metal shunt element is assumed. As a conceptual aid, each shunt element is treated as a series-parallel combination of tubes of maximum radius σ. Then the impedance of a shunt element is approximately resistive and frequency independent provided that (ref. 6)

$$\sigma < \sqrt{\frac{\mu}{\rho\omega}} \tag{C1}$$

For an absolute viscosity μ of 1.57×10^{-5} pound-second per foot^2 (7.52×10^{-4} N - sec/m^2) (JP-4 fuel at 79° F), a frequency ω of $80\times2\pi$ radians per second, and a density ρ of 1.50 slugs per foot^3 (7.73×10^2 kg/m^3) (ref. 1), inequality (C1) becomes (worst case value)

$$\sigma < 1.44\times10^{-4} \text{ ft} = 0.438\times10^{-4} \text{ m} \tag{C2}$$

The manufacturer states that each porous-metal shunt element used filters out particles with a maximum dimension greater than 4.17×10^{-5} foot (1.27×10^{-5} m). The right side of inequality (C2) is 6.9 times this amount. If it is now assumed that the effective maximum tube radius of the pores in each shunt element σ is within 6.9 times the largest dimension of the filtered particles, it follows that the condition set by inequality (C1) is satisfied. Therefore, the impedance of each porous-metal shunt element is approximately resistive and frequency independent.

For this reason, the value of the resistance R_s can be determined from curves of static-pressure drop plotted against flow rate (nearly linear). Using this method yields a value of R_s of 4.05×10^{7} pound-second per foot^5 (6.85×10^{10} N-sec/m^5).

Comparison of Shunt-Element Resistance with Shunt-Assembly Impedance

The impedance of each shunt assembly (fig. 2(a)) is

$$Z_s = R_s + j\left(\omega L_s - \frac{1}{\omega K_s}\right) \tag{C3}$$

where each assembly is treated as a lumped parameter series acoustic circuit consisting of the resistance of the porous-metal shunt element R_s, the compliance of the accumulator K_s, and the inertance of the mass of fluid L_s. It will be shown that the value of Z_s is approximately that of R_s over the frequency range of the experiment.

Compliance

The compliance of the accumulator (from ref. 6) is

$$K_s = \frac{-d\Omega}{dp} \tag{C4}$$

For a perfect gas and an adiabatic process

$$p\Omega^{\gamma} = M \tag{C5}$$

Equations (C4) and (C5) give

$$K_s = \frac{1}{\gamma} \frac{\Omega}{p} \tag{C6}$$

Taking the gas volume Ω and the absolute pressure of the gas in the accumulator p as the mean volume Ω_m and absolute mean test line pressure p_m, respectively, gives

$$K_s = \frac{\Omega_m}{\gamma p_m} \tag{C7}$$

The accumulator was brought from its initial charged state to its mean test state isothermally. This procedure yields

$$\Omega_m = \frac{p_g}{p_m} \Omega_g \tag{C8}$$

Substituting equation (C8) into equation (C7) gives

$$K_s = \frac{\Omega_g p_g}{\gamma p_m^2} \tag{C9}$$

The minimum value of shunt-accumulator compliance calculated from equation (C9) for the runs was

$$K_s \geq 1.22 \times 10^{-7} \text{ ft}^5/\text{lb} = 7.21 \times 10^{-11} \text{ m}^5/\text{N} \tag{C10}$$

The minimum frequency used in the experiment was 0.5 cps. Use of this value yields the maximum magnitude of impedance due to the compliance of the accumulator as

$$\frac{1}{\omega K_s} < 2.61 \times 10^6 \text{ lb-sec/ft}^5 = 4.41 \times 10^9 \text{ N-sec/m}^5 \tag{C11}$$

The ratio of this impedance to the resistance of a typical porous-metal shunt element is less than 6.5×10^{-2} over the frequency range studied; for frequencies of 7 cps or greater, its maximum value is less than 4.7×10^{-3}. Therefore, the compliance of the shunt accumulator K_s can be neglected.

Inertance

From reference 6, the inertance due to nonviscous fluid of density ρ in a line of length h and cross-sectional area A is

$$L = \rho \frac{h}{A} \tag{C12}$$

Adding the maximum inertance of each section of a single shunt assembly in series (excluding that in the porous-metal disk already shown to be negligible) and using 80 cps indicated that the magnitude of the impedance due to the inertance of the shunt assembly is

$$\omega L_s < 6.9 \times 10^5 \text{ lb-sec/ft}^5 = 1.17 \times 10^9 \text{ N-sec/m}^5 \tag{C13}$$

It follows that the ratio of the inertive impedance to the resistance of a shunt assembly is less than 1.8×10^{-2} over the frequency range tested. Therefore, the inertance of each shunt assembly L_s can be neglected.

Distributed Line Impedance

The impedance of each porous-metal shunt assembly is essentially resistive. Therefore, from the values given herein

$$G_D = \frac{1}{R_s} \frac{n}{\ell A} = 1.24 \times 10^{-8} \text{ ft}^4/\text{lb-sec} = 2.40 \times 10^{-11} \text{ m}^4/\text{N-sec} \tag{C14}$$

$$L_D = \frac{\rho}{A} \text{ (see eq. (C12))} = 3.62 \times 10^2 \text{ lb-sec}^2/\text{ft}^6 = 2.01 \times 10^6 \text{ N-sec}^2/\text{m}^6 \tag{C15}$$

and the effective distributed compliance of the line K_D is the same as the distributed compliance for the line with no shunt assemblies C_D. From reference 6

$$C_D = \frac{1}{L_D a^2} = 1.80 \times 10^{-10} \text{ ft}^4/\text{lb} = 3.49 \times 10^{-13} \text{ m}^4/\text{N} \tag{C16}$$

LOSSY-TUBE SHUNT ASSEMBLIES

Impedance of Lossy-Tube Shunt Elements

In order to calculate the impedance of a lossy-tube shunt element, the disturbance flow through a lossy tube is assumed to be laminar. For laminar disturbance flow, reference 4 gives

$$-\frac{\partial P}{\partial \xi} = R_\tau U + j\tau L_\tau U \tag{C17}$$

where (1) U is the complex amplitude of the sinusoidal-perturbation velocity in the axial direction averaged over a cross-sectional area of a tube, (2) the distributed specific inertance of one tube is

$$L_\tau = \frac{\rho\sqrt{\frac{\rho\omega}{2\mu}}\left(2\sqrt{\frac{\rho\omega}{2\mu}} + I_y - I_x\right)}{\left(\sqrt{\frac{\rho\omega}{2\mu}} - I_x\right)^2 + \left(\sqrt{\frac{\rho\omega}{2\mu}} + I_y\right)^2} \tag{C18}$$

(3) the distributed specific disturbance-resistance of one tube is

$$R_\tau = \frac{-\rho\omega\sqrt{\frac{\rho\omega}{2\mu}}\left(I_x + I_y\right)}{\left(\sqrt{\frac{\rho\omega}{2\mu}} - I_x\right)^2 + \left(\sqrt{\frac{\rho\omega}{2\mu}} + I_y\right)^2} \tag{C19}$$

and (4) I_x and I_y are expressed in terms of the Bessel-Kelvin functions of the first kind as, respectively,

$$I_x = \frac{-2}{r}\,\frac{\mathrm{ber}_1\left(r\sqrt{\frac{\rho\omega}{\mu}}\right)\mathrm{ber}_0\left(r\sqrt{\frac{\rho\omega}{\mu}}\right) + \mathrm{bei}_1\left(r\sqrt{\frac{\rho\omega}{\mu}}\right)\mathrm{bei}_0\left(r\sqrt{\frac{\rho\omega}{\mu}}\right)}{\mathrm{ber}_0^2\left(r\sqrt{\frac{\rho\omega}{\mu}}\right) + \mathrm{bei}_0^2\left(r\sqrt{\frac{\rho\omega}{\mu}}\right)} \tag{C20}$$

and

$$I_y = \frac{2}{r}\,\frac{\mathrm{ber}_1\left(r\sqrt{\frac{\rho\omega}{\mu}}\right)\mathrm{bei}_0\left(r\sqrt{\frac{\rho\omega}{\mu}}\right) - \mathrm{bei}_1\left(r\sqrt{\frac{\rho\omega}{\mu}}\right)\mathrm{ber}_0\left(r\sqrt{\frac{\rho\omega}{\mu}}\right)}{\mathrm{ber}_0^2\left(r\sqrt{\frac{\rho\omega}{\mu}}\right) + \mathrm{bei}_0^2\left(r\sqrt{\frac{\rho\omega}{\mu}}\right)} \tag{C21}$$

The complex amplitude of volume flow rate at a point along the length of a tube is

$$V = U\pi r^2 \tag{C22}$$

Combining equations (C17) and (C22) gives

$$-\frac{\partial P}{\partial \xi} = \left(\frac{R_\tau}{\pi r^2} + j\omega \frac{L_\tau}{\pi r^2}\right) V \tag{C23}$$

The ratio of tube length d to wavelength was less than 0.003 for the frequencies of the experiment. For this reason the right side of equation (C23) is taken as independent of ξ. (This is equivalent to taking the distributed shunt compliance of each lossy tube as zero.) The difference in pressure amplitude across the length of a tube at a given frequency is then

$$\Delta P = \left(\frac{R_\tau d}{\pi r^2} + j\omega \frac{L_\tau d}{\pi r^2}\right) V \tag{C24}$$

Each shunt element contained 21 tubes in parallel. From equation (C24), the lumped inertance of a shunt element is

$$L_T = \frac{L_\tau d}{21\pi r^2} \tag{C25}$$

the lumped resistance is

$$R_T = \frac{R_\tau d}{21\pi r^2} \tag{C26}$$

and the lumped impedance is

$$Z_T = R_T + j\omega L_T \tag{C27}$$

The lumped inertance L_T and the lumped resistance R_T of a lossy-tube shunt element can be evaluated for a given frequency by using tables of ber and bei functions (ref. 7). The values of the parameters used to obtain L_T and R_T were

$\rho = 1.50$ slugs/ft^3 = 7.73×10^2 kg/m^3
r = 3.06×10^{-4} ft = 0.933×10^{-4} m
$\mu = 1.54\times10^{-5}$ lb-sec/ft^2(JP-4 fuel at 85° F) = 7.38×10^{-4} N-sec/m^2
d = 0.125 ft = 3.81×10^{-2} m

The lumped resistance and inertance were essentially constant over the frequency range of the experiment with the following values, respectively:

$$R_T = 2.66\times10^7 \text{ lb-sec/ft}^5 = 4.50\times10^{10} \text{ N-sec/m}^5$$

and

$$L_T = 4.04\times10^4 \text{ lb-sec}^2\text{/ft}^5 = 6.84\times10^7 \text{ N-sec}^2\text{/m}^5$$

A calculation using the method given in the porous-metal shunt-element section of this appendix showed that the impedance of the rest of the lossy-tube shunt assembly (accumulator, tubing, etc., fig. 2) was negligible compared with that of the lossy-tube shunt elements.

Distributed-Line Impedance

From equation (C27) the effective distributed shunt admittance including the shunt compliance of the main line C_D is

$$Y_D = G_D + j\omega K_D \tag{C28}$$

where the effective distributed leakage is

$$G_D = \frac{n}{\ell_A} \frac{R_T}{R_T^2 + \omega^2 L_T^2} \tag{C29}$$

and the effective distributed shunt compliance of the line is

$$K_D = C_D - \frac{n}{\ell_A} \frac{L_T}{R_T^2 + \omega^2 L_T^2} \tag{C30}$$

The distributed inertance of the line L_D is the same as that for the porous-metal shunt element case (eq. (C15)). The value of C_D is given by equation (C16).

REFERENCES

1. Regetz, John D., Jr.: An Experimental Determination of the Dynamic Response of a Long Hydraulic Line. NASA TN D-576, 1960.

2. Blade, Robert J.; Lewis, William; and Goodykoontz, Jack H.: Study of a Sinusoidally Perturbed Flow in a Line Including a 90° Elbow with Flexible Supports. NASA TN D-1216, 1962.

3. Lewis, William; Blade, Robert J.; and Dorsch, Robert G.: Study of the Effect of a Closed-End Side Branch on Sinusoidally Perturbed Flow of Liquid in a Line. NASA TN D-1876, 1963.

4. Holland, Carl M.; Blade, Robert J.; and Dorsch, Robert G.: Attenuation of Sinusoidal Perturbations Superimposed on Laminar Flow of a Liquid in a Long Line. NASA TN D-3099, 1965.

5. Terman, Frederick.: Radio Engineers' Handbook. McGraw-Hill Book Co., Inc., 1943.

6. Kinsler, Lawrence E.; and Frey, Austin R.: Fundamentals of Acoustics. John Wiley & Sons, Inc., 1950 (first edition).

7. Nosova, Liubov N. (Prasenjit Basu, trans.): Tables of Thomson Functions and Their First Derivatives. Pergamon Press, 1961.